ANALYSIS OF THE INFLUENCE OF THE DIFFERENT VARIABLES INVOLVED IN A DAMAGE PROGRESSION PROBABILITY MODEL

Campos, A.[1], Castillo, C.[1] and Molina, R.[2]

Nowadays risk based designs as well as reliable maintenance strategies are essential when dealing with coastal structures. In that sense, the probability of failure due to hydraulic instability of the armor layer is one of the main issues in rubble mound breakwaters, and so is improving the knowledge on the deterioration rate of the armor layer. In 2012 Castillo et al. made some suggestions on how to build consistent stochastic damage models and proposed a comprehensive Damage Progression Probability Model (DPPM) with general validity, depending on a pair of parameters for each of the three major entities involved in the problem: structure, wave action and initial damage. Based on experimental data, two different calibrations of these parameters are accomplished in the present paper, allowing an initial evaluation of the specific influence of each entity in the model.

1. INTRODUCTION

In many countries, development has been historically connected to maritime trade inside and outside the borders. Economies of scale have favored even more sea transport and, thanks to the increase in ship's dimensions, approximately 90% of the worldwide trade is carried out nowadays through the oceans, according to the United Nation Conference on Trade And Development (UNCTAD) in 2014. On the one hand, this trend suggests a demand of port's facilities at greater depths (more exposed to wave action), which are needed for admitting large bulk carriers. But, on the other hand, the lack of investment as a consequence of a current unbalanced economical system evidences the urge for reliable maintenance policies in order to guarantee the functionality of the already-built ones.

In the last few years, some damage episodes in coastal defenses together with the increasing concern due to clear evidences on climate change (such us sea level rise or modification of intensity and direction of storms according to the Intergovernmental Panel on Climate Change, IPCC), highlight even more the importance of breakwaters and the huge economical and human repercussions associated to both their construction and their loss of functionality. As a consequence, Port's Authorities are more and more interested in evaluating the damage caused by past storms or in estimating the effects of a future one. This is especially manifest in rubble mound breakwaters due to their reshaping nature and evolutionary response, which are hitherto the most extended breakwater typology in most parts of the world. As an example in Spain, the country of the European Union with the longest coastline (7880 km), 83% of the about 200km of breakwaters in 2001 were rubble mounds whereas just 8% were vertical at that time, according to Negro et al. (2001). Despite vertical breakwaters may represent a better alternative in terms of performance, total costs, quality control, environmental aspects, construction time and maintenance, this typology was almost abandoned in the thirties in most countries (with the exception of Japan and Italy) in favor of the rubble mound type after several vertical breakwater collapses (Oumeraci, 1994). Thus, it is essential to develop tools for assisting conservation of rubble mound breakwaters.

Breakwater failure can occur due to a system of different failure modes, which should be firstly identified in order to provide a reliable design. Traditionally they are considered as independent; but the combination or relations among them could be especially relevant when applying probability or probability-safety factor design methods (Campos et al., 2010). Among all these possible failure modes, seaside armor layer hydraulic stability is probably the most critical to the integrity and functionality of a traditional rubble mound breakwater. Wave forces might provoke armor unit movements such as rocking, displacement of units out of the armor layer, sliding of a whole blanket or settlement due to compaction. The complicated highly non-linear flow over the slope, involving wave breaking, together with the variable shape of armor units and their random placement, make practically impossible to achieve analytical expressions for the calculation of actions and reactions, and thus, to determine instantaneous armor unit stability. That is the reason why stability formulae is historically empirical or semi-empirical, associated with experimental results relating the response of the armor layer to parameters of the incident wave train and breakwater characteristics, and ideally improved with

prototype observations. Since the pioneering works of the Spanish de Castro (1933) and Iribarren (1938), several stability models have been proposed and many hundred studies on breakwater armor layer stability have been published. That gives an idea on the relevance of this failure mode; however, the achievement of a unique formula seems to be rather difficult.

First hydraulic stability models, from which Hudson's (1958) is the most disseminated, were aimed to characterize the initiation of movement. Their general structure is expressed in Eq.1: the stability of the armor layer is defined to be reached when the stability number (N_S) is lower than a certain function (*f*) depending on the n parameters influencing stability ($p_1, p_2,..., p_n$) and an empirical coefficient *(K)* representing the parameters not accounted for in the stability equation (Hald, 1998):

$$N_S = \frac{H}{\Delta D_{n50}} < f(K, p_1, p_2,..., p_n) \qquad (1)$$

During the 70's and 80's there was an intensive research on the stability of rubble mound breakwaters: Ahrens and McCartney (1975), Thompson and Shuttler (1975), Losada and Giménez-Curto (1979)... But probably the most innovative advance corresponds to Van der Meer (1985), who proposed two well-known stability formulae, specific for plunging waves and for surging waves, including the influence of wave height (*H*), wave period (by means of Iribarren's number, ξ_0), number of waves (N_w), equivalent cube length (D_{n50}), relative excess specific weight (Δ), breakwater slope (*cotα*) and permeability of the core (*P*). Furthermore, the well-known quantitative damage level parameter (*S*) suggested by Broderick and Ahrens (1982) (see Eq.2) was introduced in the formulae, and thus, it can be regarded as the first damage progression model.

$$S = \frac{A_{eroded}}{D_{n50}^3} \qquad (2)$$

Van der Meer related the Hudson's "no-damage" criteria and filter exposure (failure criteria) to different values of S depending on breakwater slope. However, it presents some limitations as a damage progression model: it tends to overestimate damage for more than 8000 waves and it is not designed to include the cumulative effect of previous storms.

Motivated by the need of predicting damage evolution on rubble mound breakwaters and to extend the validity of the results to the long-term (which is the basis for reliable maintenance programs, risk-based designs or decision-making tools), further damage progression models were developed: Teisson (1990), Kaku et al. (1991), Medina (1996), Gómez-Martín and Medina (2004)... Probably the most disseminated attempt of the last decades on this matter was accomplished by Melby and Kobayashi (1998), referred as M&K herein. They carried out physical experiments with depth limited random waves considering, not only the long-term, but also the variation in storm sequences. What is more, the variability of damage was also addressed by means of analytical expressions characterizing the total range of variation of the damage descriptors during the experiments. However, they did not provide the complete Probability Density Functions (PDF) needed for a more precise analysis of damage progression, i.e. they did not provide the distribution of damage around a predicted mean value of the damage progression model.

This fact, as well as some modeling difficulties reported by M&K (1999), motivated Castillo et al. (2012) to make some suggestions on how to build consistent stochastic models avoiding the selection of easy-to-use mathematical functions, which were replaced by those resulting from a set of properties to be satisfied by the model. Contrary to other existing models that are built under a deterministic approach, the Cumulative Density Function (CDF) of Eq.3 was proposed after applying dimensional analysis (Buckingham Π theorem), compatibility conditions and the central limit theorem. The Damage Progression Probability Model of Castillo et al. (2012), referred as DPPM herein, was developed under assumptions of general validity but their variables need to be calibrated for each specific case.

$$F_{D^*(t^*)}(x) = \Phi\left(\frac{(x-\gamma)^{1/b} - \mu_0 - kt^*}{\sqrt{\sigma_0^2 + rt^*}} \right) \qquad (3)$$

, where γ and *b* are breakwater dependent, *k* and *r* include wave action, μ_0 and σ_0 depend on the initial damage conditions and t^* is the relative duration. Notice that damage D^* is proven not to be normal.

The DPPM permits to account, not only for the stochastic nature of wave climate, but also for the uncertainties derived from the construction process, from the system response itself and for the deterioration rate. Thus, it is a mathematical tool that might improve the probabilistic approach in breakwater design and conservation strategies. Probabilistic methods are well established in coastal engineering (see Burcharth, 1997, Castillo et al., 2004, 2006, Mínguez et al., 2006…) and methodologies for reliability based designs are present in design codes such as the European PROVERBS (Oumeraci et al., 1999), the Spanish ROM 0.0-01 (Puertos del Estado, 2001) or the North American CEM (U. S. Army Corps of Engineers, 2002). However, while most efforts have been made in characterizing the randomness of wave climate, the structural response is still considered as deterministic or pseudo-deterministic in most cases. Wave climate is typically addressed by monitoring on-site, modeling and predicting. Based on that, the DPPM should necessary be complemented, not only with physical testing, but also with prototype monitoring. Thanks to the recent advances and affordability of non-intrusive drones, scanning technologies, photogrammetric restitutions..., Port's Authorities have nowadays tools to monitor their structures in order to evaluate the state of the breakwater after a certain storm (see Figure 1). That would help to develop a field database for enhancing laboratory results and, in particular, for better calibration of the DPPM.

Figure 1. Dron equiped with zeus-air (left) and scanned detail (right) of the new breakwater of San Andrés (Málaga) made with Cubipods. Images given by the company Flyviews.

Scanning tools also provide the opportunity of re-discussing the concept of "damage", i.e. to complement or re-define the damage parameter (S) proposed by Broderick and Ahrens (1982), and to settle down standards for their measurement and definition both in laboratory and in prototype. These aspects are beyond the scope of this paper. As it was stated by many authors, there is a lack of standards in laboratory test on hydraulic stability of rubble mound breakwaters. Reproducibility of most experiments is either complicated or impossible, mainly due to the huge amount of parameters, methodologies, measurement techniques, post-processing strategies... that need to be described for that purpose, and which are not always available on literature. A description of these peculiarities is given in Campos (2014). What is more, repeatability of damage tests is also quite atypical taking into account that armor layer placement and response are random variables themselves. Thus, repetition of damage experiments is a must.

In the present lines, two initial calibrations of the DPPM are accomplished: the first one is based on the damage results from M&K and the second one is based on a set of experiments carried out at the Harbour Research Laboratory (HRL) of the Polytechnic University of Madrid, in which a structured light scanner was used for measuring damage. The results allow an initial evaluation of the influence of each parameter in the DPPM.

2. DPPM CALIBRATION USING M&K (1998) RESULTS

As it was mentioned before, one of the basis for developing the DPPM of Eq.3 was the application of dimensionless analysis by means of the Buckingham Π theorem. Castillo et al. (2012) ended up with six ratios affecting dimensionless damage (D^*): relative specific weight ($\Delta^* = (\gamma_a - \gamma_w)/\gamma_w$), breakwater rubble mound slope (α^*), relative still water depth ($h^* = h_t/D_{n50}$), initial dimensionless damage (D_0^*), stability number ($N_s^* = H/\Delta \cdot D_{n50}$) and relative duration ($t^* = t/T_m$). First triad is considered fixed in the DPPM, whereas second triad is variable (see Eq.4):

DIMENSIONLESS RATIOS: Fixed in the DPPM   Variable in the DPPM

$$D^* = h \left(\overbrace{\Delta^*, \quad \alpha^*, \quad h^*}, \quad \overbrace{D_0^*, \quad N_S^*, \quad t^*} \right) \qquad (4)$$

PARAMETERS OF THE DPPM: γ, b μ_0, σ_0 k, r t^*

The DPPM was developed following assumptions of general validity and, consequently, their parameters need to be particularized for each specific case. This is especially evident for the various types of armor units, each of which has different mechanism of damage initiation, different interaction with waves or even a different way of defining what is considered as "damage". The present paper is just focused on some examples with scaled quarry stones, using the damage descriptor proposed by Broderick and Ahrens (1982).

Damage progression models usually describe just mean damage evolution and assumes a normal distribution of damage when adapting the formulation for a probabilistic approach. However, according to the DPPM, damage does not have a normal distribution, but transformed damage $D_{trans}=(D-\gamma)^{1/b}$ does.

The median and variance of the non-transformed damage can be derived from Eq.3, as it is shown respectively in Eq.5 and Eq.6. By comparing these values with the experimental mean and variance, the goodness of fit of the DPPM can be calculated. In this case, the individual error derived from each damage measurement is defined according to Eq.7, where W_1 and W_2 are weighting coefficients. As an initial approach, both weights have been assigned a value of 1. The total error along the damage progression curve is considered here as a mean value of the n individual errors derived from each damage measurement.

$$\mu_{DPPM} = \left(\mu_0 + kt^* \right)^b + \gamma \qquad (5)$$

$$\sigma_{DPPM} = \left(\sqrt{\sigma_0^2 + rt^*} + \mu_0 + kt^* \right)^b - \left(\mu_0 + kt^* \right)^b \qquad (6)$$

$$Error = \frac{\sum_{i=1}^{i=n} error_i}{n} \qquad (7)$$

$$error_i = \sqrt{\frac{W_1 \left(\mu_{measured,i} - \mu_{DPPM,i} \right)^2 + W_2 \left(\sigma_{measured,i} - \sigma_{DPPM,i} \right)^2}{W_1 + W_2}} \qquad (8)$$

For completing and initial calibration of the DPPM, experimental data of M&K is utilized, in particular the results from Series A (long term experiment). Two similar rubble mound sections were tested at the same time, composed of a core, a double layered filter and a double layered armor layer with quarry-stones of D_{n50}=3.64cm, uniformly graded, at a 2H:1V slope. The models were exposed to depth limited irregular waves following a TMA spectrum, using a wave paddle without dynamic absorption system in a wave flume, during intervals of 15 minutes. Damage was measured after 30 min of testing, by means of 8 profiles per section, which were considered as independent damage magnitudes after calculating the damage descriptor according to Eq.2. Each wave condition was tested until a damage equilibrium was visually appreciated. At that moment, a new wave condition (more energetic) started to be generated until the filter is exposed. This stopping criteria is analogous to the concept of *Initiation of Destruction* introduced by Vidal et al. (1991).

The dimensionless variables successively tested in Series A of M&K are summed up in Table 1. Notice that water depth was increased at the middle of the experiment. Regarding that the DPPM was developed assuming a constant value of the relative still water depth, the whole Series A was divided into an Initial Section (lower water depth) and a Final Section (higher water depth). Each section was used independently for the calibration process.

For the calibration of the parameters of the DPPM, a bound constrained optimization code was implemented in the computing environment of Matlab®, in particular the fminsearchbnd algorithm developed by Jonh D'Errico. As it was said before, the optimization process is not aimed to minimize

the error of the DPPM derived from each individual damage measurement, but the mean error along the whole damage progression curve. Because of that, the breakwater parameters γ and b on Eq.3 need to be fixed on each iteration for the whole damage progression curve, whereas the rest of parameters are variable. Eq.3 have been applied step-by-step, which means that t^* represents the relative duration between two measurements, rather than the accumulated total relative duration. This approach leads to two consequences:

- The wave action parameters, k and r, need to be forced to have a constant magnitude for the same value of N_S.
- The initial damage parameters, μ_0 and σ_0, are optimized just for the first damage measurement. For the rest, the calculated $\mu_{DPPM,i}$ and $\sigma_{DPPM,i}$ (Eq.5 and Eq. 6) for the measured damage D_i are straightly the parameters μ_0 and σ_0 for the measured damage D_{i+1}.

CASE	Δ^*	α^*	h^*	N_s^*	t^*	Nº of measurements
1				1.55	1022.7	3
2			3.28	1.92	1065.1	3
3	1.66	0.46		2.18	1034.5	15
4				1.67	1040.5	2
5			4.33	2.15	1077.8	11
6				2.47	1084.3	21

Table 1. Dimensionless variables successively tested in Series A of M&K

CASE	γ	b	k (N$_{S1}$)	k (N$_{S2}$)	k (N$_{S3}$)	r (N$_{S1}$)	r (N$_{S2}$)	r (N$_{S3}$)	μ_0	σ_0	Error
MK1_01	-1.098	0.291	0.0099	0.0323	0.0392	0.8266	9.1811	15.028	1.0990	0.2031	0.1614
MK1_02	0.021	**0.500**	0.0010	0.0017	0.0017	0.0043	0.0135	0.0135	0.9805	0.0715	0.1710
MK1_03	-0.699	**0.400**	0.0026	0.0055	0.0055	0.0335	0.1392	0.1881	1.0052	0.1081	0.1651
MK1_04	-1.436	**0.300**	0.0151	0.0340	0.0371	0.7872	8.2253	12.548	0.8086	0.3863	0.1629
MK1_05	-1.148	**0.250**	0.0255	0.0733	0.1277	4.3921	74.666	214.54	0.8257	0.4918	0.1670
MK1_06	**0.000**	0.360	0.0022	0.0063	0.0067	0.0238	0.3773	0.3785	0.3540	0.9849	0.1639
MK1_07	**0.000**	**0.500**	0.0008	0.0017	0.0018	0.0053	0.0128	0.0132	1.2698	0.3974	0.1767
MK1_08	**0.000**	**0.400**	0.0012	0.0040	0.0043	0.0139	0.0753	0.1473	1.1180	0.2219	0.1674
MK1_09	**0.000**	**0.300**	0.0030	0.0105	0.0197	0.0869	1.8132	4.6841	0.0419	0.2234	0.1668
MK1_10	**0.000**	**0.250**	0.0049	0.0206	0.0644	0.7353	10.076	81.334	0.9609	0.5026	0.1821

Table 2. Optimized parameters of Eq.3 based on the experimental results of M&K, Series A, Initial Section (lower water depth). Bold characters are fixed values in the optimization process

CASE	γ	b	k (N$_{S4}$)	k (N$_{S5}$)	k (N$_{S6}$)	r (N$_{S4}$)	r (N$_{S5}$)	r (N$_{S6}$)	μ_0	σ_0	Error
MK2_01	2.582	0.213	0.0131	0.1548	2.1470	528.60	5617.8	207313	6.1445	0.9244	0.2108
MK2_02	2.444	**0.500**	0.0004	0.0016	0.0036	0.0426	0.0618	0.0839	5.8666	0.8806	0.3003
MK2_03	2.776	**0.400**	0.0034	0.0034	0.0121	0.0244	0.5791	1.6956	5.6552	1.2490	0.2731
MK2_04	2.896	**0.300**	0.0004	0.0137	0.0842	0.0751	16.850	155.28	6.0965	1.2917	0.2382
MK2_05	2.564	**0.250**	0.0461	0.0492	0.4426	62.225	340.16	5930.8	5.5472	0.8931	0.2143
MK2_06	**0.000**	0.242	0.1047	0.3011	1.4366	296.67	5326.8	46076.	5.8185	1.1662	0.2331
MK2_07	**0.000**	**0.500**	0.0011	0.0026	0.0047	0.1174	0.1174	0.1174	5.7014	0.0126	0.3189
MK2_08	**0.000**	**0.400**	0.0036	0.0080	0.0190	0.0456	1.7718	2.8382	5.8172	1.1857	0.2908
MK2_09	**0.000**	**0.300**	0.0102	0.0533	0.1793	6.9361	114.30	465.03	5.8712	1.1511	0.2585
MK2_10	**0.000**	**0.250**	0.1054	0.2204	1.0327	94.561	2922.1	21800.	5.7854	1.2016	0.2363

Table 3. Optimized parameters of Eq.3 based on the experimental results of M&K, Series A, Final Section (higher water depth). Bold characters are fixed values in the optimization process

The results from fitting Eq.3 into the Initial Section and the Final Section of Series A are summarized in Tables 2 and 3 respectively. Ten different cases are presented for each Section, derived from fixing b, γ or both during the optimization process. After analyzing this information, the following conclusions can be extracted:

- The initial damage parameters, μ_0 and σ_0, allow the characterization of damage progression in damaged structures, as it clearly shows the results of the Final Section of Series A. Even at the Initial Section, it can be observed that the DPPM predicts a certain initial damage, which might be indeed expectable due to the natural randomness of the construction process.

- The wave action parameters, k and r, have been directly optimized for each interval of constant N_S. Nevertheless, more research is needed for straightly calculating both parameters as a function of N_S, or even to find analytical relationships between them. The influence of the stability number on damage, has been traditionally defined following a potential trend: $a_s(N_S)^\beta$. Melby (1999) indicates that, in M&K damage progression model, the empirical coefficient a_s is related to the breakwater slope and the permeability among others. According to the results herein, it seems that there is also a dependency of k and r on breakwater's parameters, as they tend to increase when decreasing b.

- From the breakwater parameters, γ is a location parameter that helps to enhance the goodness of fit, but relatively good approximations are also obtained when fixing $\gamma=0$. On the other hand, b is able to modify the damage progression trend, and thus, it seems to be related to the way damage evolves. This shown in Figure 2 and Figure 4: for $b=0.5$ damage progression is more linear and less likely to stabilize, whereas for $b=0.25$ damage tends to a faster stabilization and, consequently, to show a sharper exponential trend. As a reference, Melby (1999) stated that Van der Meer's data suggests a coefficient of $b=0.5$, but a value of $b<0.5$ for more than 8500 waves. Indeed M&K proposed $b=0.25$ in their model. According to the results herein, the optimum values of b are 0.29 for the Initial Section (see Figure 3) and 0.21 for the Final Section (see Figure 5) of Series A.
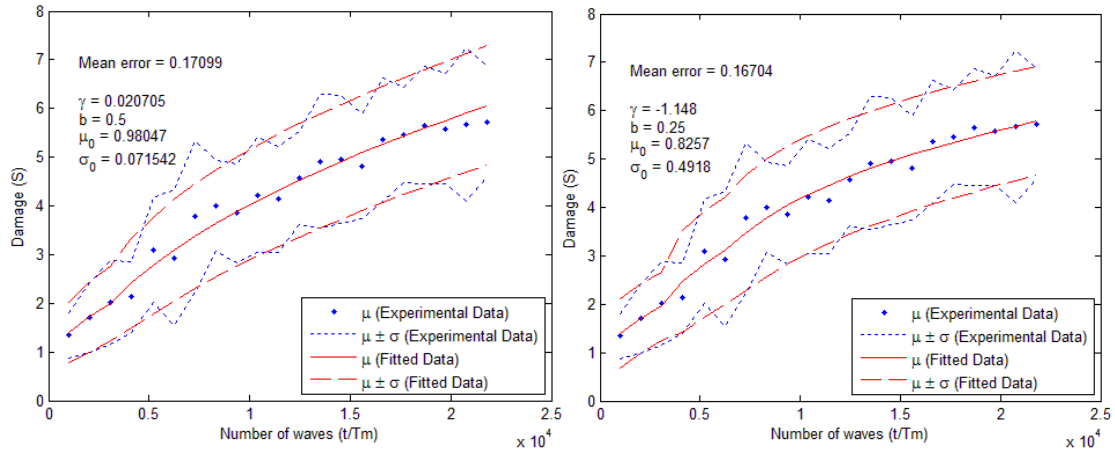

Figure 2. Graphic results from the fitting process of Case MK1_02 (left) and Case MK1_5 (right), based on the experimental results from M&K(1998), Series A, Initial Section (lower water depth).
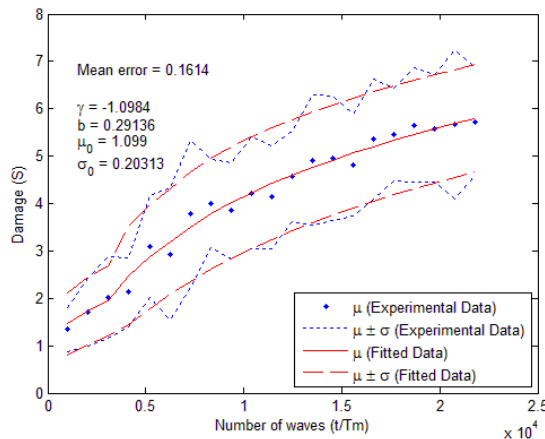

Figure 3. Graphic result from the fitting process of the optimum case (MK1_01), based on the experimental results from M&K(1998), Series A, Initial Section (lower water depth).
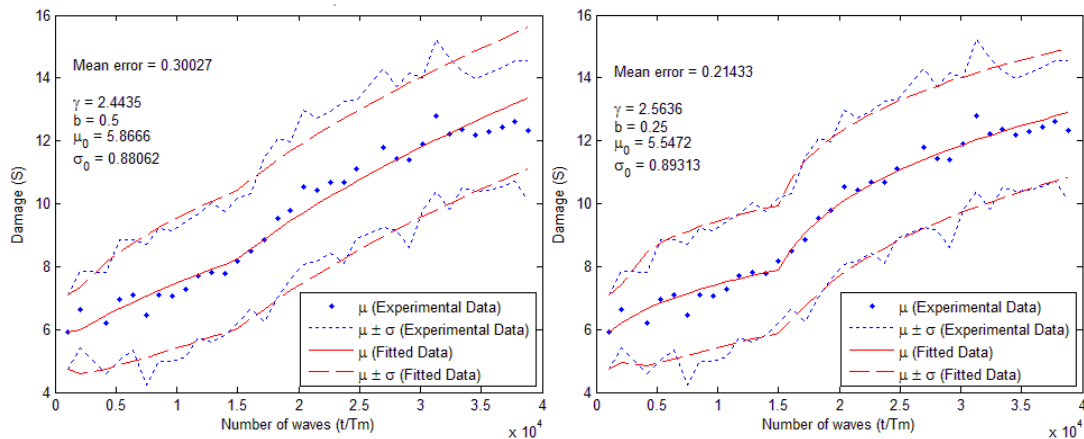
Figure 4. Graphic results from the fitting process of Case MK2_02 (left) and Case MK2_5 (right), based on the experimental results from M&K(1998), Series A, Final Section (higher water depth).
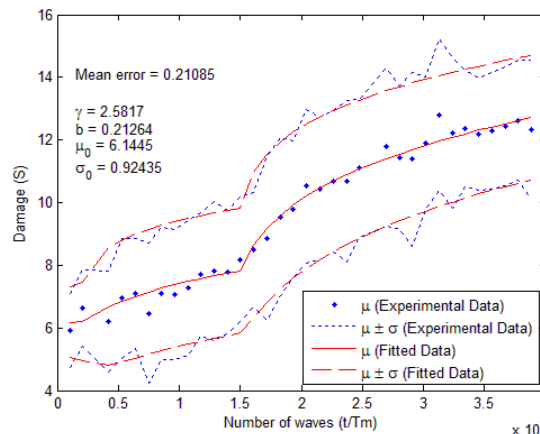

Figure 5. Graphic result from the fitting process of the optimum case (MK2_01), based on the experimental results from M&K(1998), Series A, Final Section (higher water depth).

3. DDPM CALIBRATION UNDER A DIFFERENT APPROACH

A further calibration of the DPPM has been accomplished using a set of experiments carried out at the wave flume of the Harbour Research Laboratory (HRL) of Madrid, which are described in more detail in Campos (2014). These tests present some similarities with M&K's and complete them, but show three main conceptual differences:

- Rather than working with depth limited conditions, which introduces non-linear processes and complicates the characterization of wave-structure interaction, wave breaking is attempted to be avoided in order to facilitate reproducibility and interpretation of the results. Figure 6 compares the location of M&K wave cases in the diagram of Le Méhauté (1976) with the ones from the HRL. Despite not reaching the breaking limit in the diagram, some of the highest waves of the more energetic spectrum of the HRL's wave cases were observed to break before reaching the model.

- In damage accumulation experiments, the model is usually exposed to a series of sea states with increasing energy until the structure reaches a certain level of damage. In many cases, the energy steps are established by fixing T_p and increasing H_S. But this approach is not in consonance with natural processes, where the increment in wave height is normally accompanied by an increase in wave period. From the different alternatives for taking into account this behavior, in this case energy increasing steps have being designed by maintaining a steepness of 0.04 (see Figure 7).

- As it was mentioned in the introduction, a notable evolution in the available tools for damage measurements is perceived in recent years. First damage tests were done using visual information and, after that, damage quantification was usually achieved by means of physical profilers. For the present study, the spatial variation of the model's geometry was characterized with a structured light 3D scanner (resolution up to 0.5mm), defining damage as the mean damage level parameter (Eq. 2) of the 1mm spacing profiles obtained from the scanned surface.
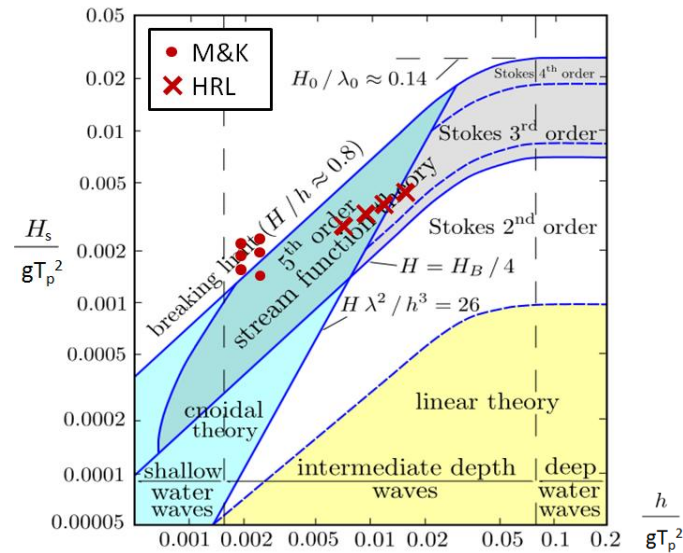
Figure 6. Location of M&K (1998) wave cases and HRL wave cases in the diagram of Le Méhauté (1976).
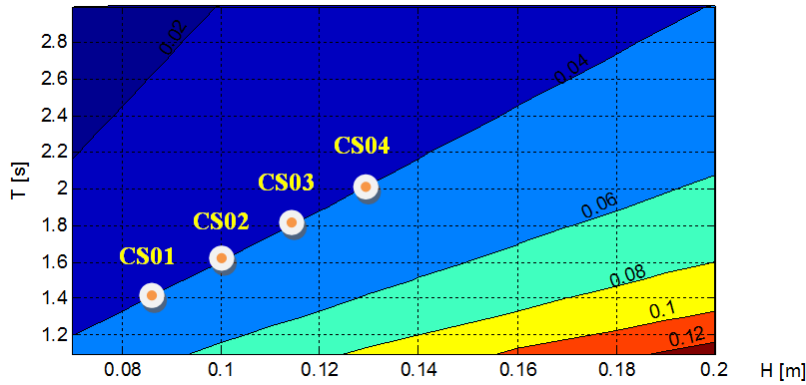

**Figure 7. Location of the HRL wave cases in a steepness isolines map for h=0.29m.**

The main objective of the experiments is to characterize damage progression variability on quarry-stone non-overtopped rubble mound breakwaters. For doing so, damage evolution is analyzed over 6 similar sections, which main characteristics are presented in Table 4 and Figure 8. The physical model consists on a section of a generic rubble mound breakwater, composed of a core, a double layered filter, and a double layered armor layer of quarry-stones (γ_a=2.65 ton/m^3) with a 2V:3H slope, steeper than the one used by M&K (1V:2H). Armor layer nominal diameter is 3.05cm, narrow graded, and with a mean length-to-thickness factor around 2 and a mean blockiness factor around 45%. After selecting the granular material, it was washed for avoiding turbidity inside the wave flume, and painted in order to help the visual interpretation of damage and to make possible the application of the visual stopping criteria: Initiation of Destruction (filter exposure). Even taking into account that the same technician built the 6 tested sections, aided by reference marks on the flume and a slope tester, and also measured the initial porosity from a snap-shot assisted by a counting software, the initial porosity measurements show a range of variation: 33.8%, 32.9%, 34.4%, 30.7%, 31.1% and 30.7%. Despite porosity is a common parameter in breakwater design, it is indeed difficult to measure and to be achieved with accuracy during the construction process. That gives an idea of the stochastic nature of the process itself and proves the existence of randomness in the initial damage.

As a peculiarity, a central divider was placed for testing two independent sections at once. Some examples on this matter can be found in Carver and Wright (1991), Medina (1992), Medina and Hudspeth (1994), Melby and Kobayashi (1998)... The divider was driven into the bottom ramp and into the retaining wall. Additional strength against buckling is provided by the physical model and a reinforcing transversal rib placed high enough for avoiding interaction with waves. The initial construction and successive reconstructions are faced independently on each side of the divider, including the core, so as to ensure an independent response of each section.

	W$_{15}$ (g)	W$_{50}$ (g)	W$_{85}$ (g)	D$_{n50}$ (cm)	D$_{n85}$ / D$_{n15}$	Rock Manual (2007) classification	LT$_{mean}$ (Aspect ratio)	BLc$_{mean}$ (Blockiness factor)
Table 4. Main characteristics of the core, filter and armor layer (quarry-stones) of the HRL damage progression tests								
Core	0.03	0.62	1.20	0.61	3.5	Quarry run gradation	-	-
Filter	3.28	4.92	6.58	1.23	1.3	Narrow gradation	-	-
Armor layer	62.8	75.4	86.1	3.05	1.1	Narrow gradation	1.9	44.9%
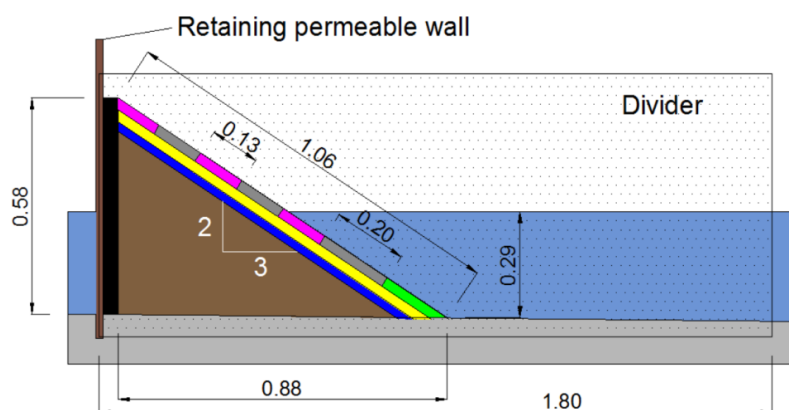
Figure 8. Sketch of the physical model tested at the HRL (dimensions in meters)

The experimental layout is shown in Figure 9. The 2D wave flume of the HRL of Madrid is 52m long per 1m wide per 1.6m high. One side is made of glass along the whole channel and, therefore, it permits straight visual inspection during the experiments. Wave conditions are generated by piston-paddle wavemaker with dynamic absorption system on. In order to provide a gradual transition to shallower waters, the seabed is flat during the first 16m beyond the paddle board and, after that, it follows a mild slope of 2% for 12m and a milder one of 1% for the lasts 11m before reaching the model. Passive absorption systems are installed at both sides of the flume, made of the polymeric porous media presented by Cabrerizo et al. (2010). Two arrays of four resistive wave gauges were used for measuring water surface variations, one allocated next to the model, and the other one close to the wave paddle. Tests are monitored by means of a lateral and an overhead camera, and damage is measured using a structured light 3D scanner.
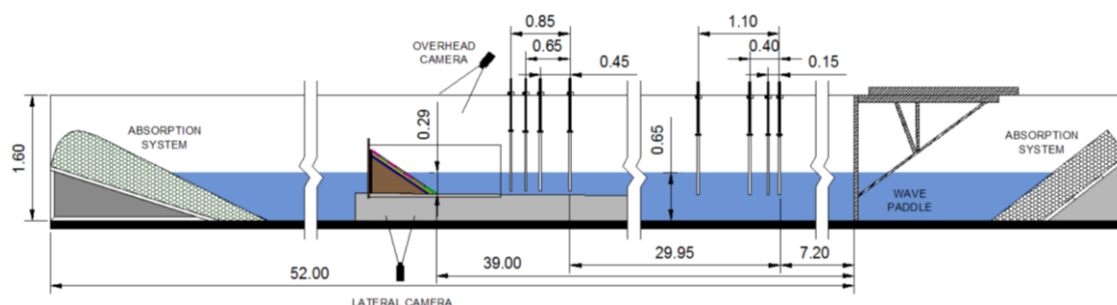
Figure 9. Experimental layout of the HRL damage progression experiments.

The model was exposed to irregular waves following a Jonswap spectrum with a peak enhancement factor of γ=3.3. Designed wave cases are summed up in Table 5, including the expected and measured wave conditions close to the wave paddle and close to the model's location. In order to provide a fully developed spectrum, but avoiding long testing durations, wave cases are tested in intervals of about 660 waves (t/T$_m$). DPPM dimensionless tested variables are shown in Table 6.

Table 5. Designed and measured incident waves cases for the HRL's damage tests							
	Design spectrum at model's location		Measured spectrum at model's location		Design spectrum at wave paddle		Measured spectrum at wave paddle	
CASE	H_S (m)	T_p (s)	H_S (m)	T_p (s)	H_S (m)	T_p (s)	H_S (m)	T_p (s)
01	0.085	1.40	0.086	1.37	0.105	1.40	0.093	1.38
02	0.100	1.60	0.102	1.56	0.115	1.60	0.104	1.55
03	0.115	1.81	0.113	1.85	0.118	1.81	0.111	1.81
04	0.130	2.02	0.127	1.97	0.120	2.02	0.118	2.00

Table 6. Dimensionless variables successively tested in HRL's damage tests					
CASE	Δ^*	α^*	h^*	N_s^*	t^*
1				1.7	1320
2	1.65	0.59	9.5	2.0	1320
3				2.3	1320
4				2.6	1320

After comparing the incident designed spectrum with the measured incident energy, it was observed that there was an excellent matching except for Case 4, the most energetic wave case. As it was aforementioned, Case 4 presents some depth limited difficulties including breaking of some of the highest waves before reaching the model. Because of that, Case 4 has not been taken into account in the DPPM calibration but just used for reaching the Initiation of Destruction. On the other hand, Case 1 barely produces displacements of a few stones and, thus, it has been used just as an stabilization wave case for reducing settlements and facilitating damage analysis.

Testing strategy is similar to M&K's: each wave case is generated until visual damage stabilization is observed. At that moment wave energy is increased until the Initiation of Destruction is reached. Damage is measured from 2 to 2 tests, i.e. after about 1320 waves. Because one of the main objectives is to characterize damage progression variability, 3 repetitions were performed, named DA1, DA2 and DA3. 2 sections are tested within each repetition. Therefore, 6 damage progression curves have been measured. The results are shown in Figure 11, together with a snap-shot associated with failure criteria.

Combining all 6 results from Figure 11, the mean damage progression curve of Figure 10 is built, which includes the associated deviation derived from each damage measurement. This curve is the one used for calibrating the DPPM.
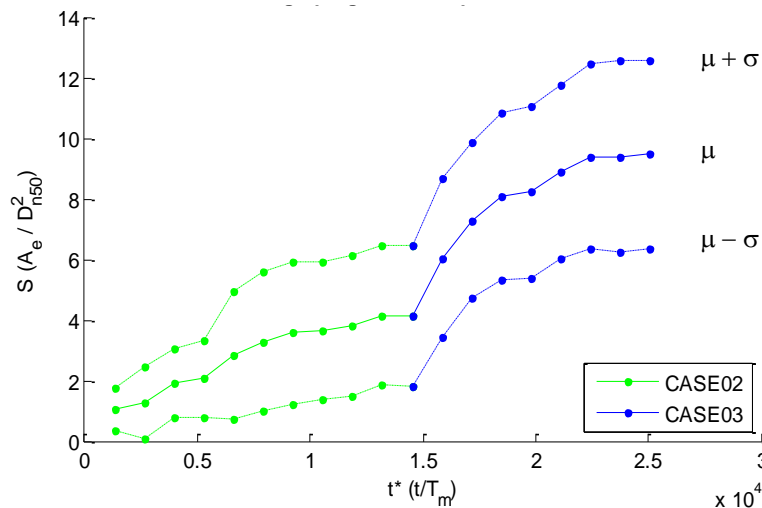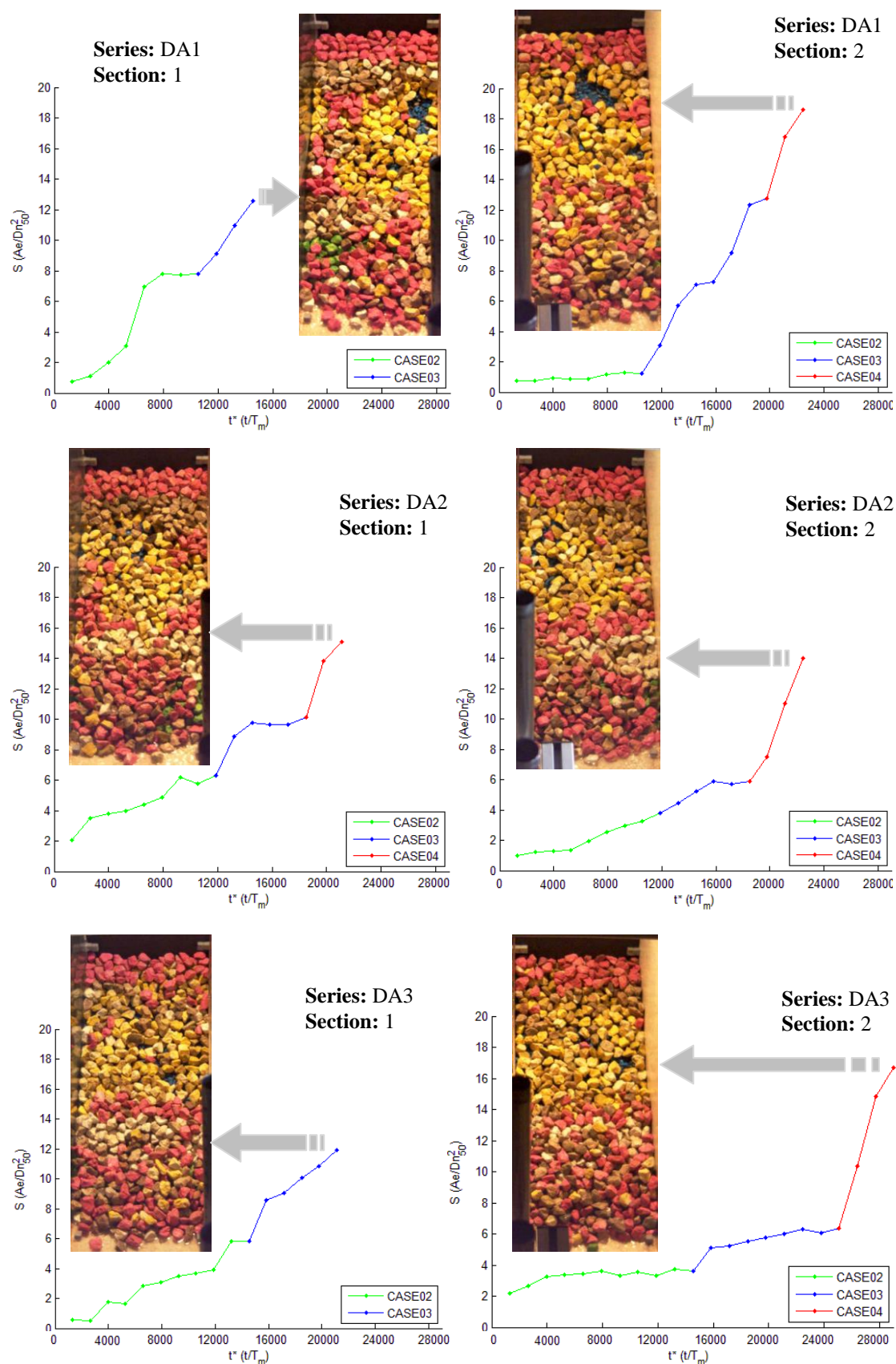

Figure 10. Experimental damage progression curve from the HRL's damage tests

Figure 11. Damage progression measured curves for the 6 sections tested at the HRL. Snap-shots correspond to the final state (Initiation of Destruction) for each case.

Comparing the measured damage progression curve of Figure 10 with Series A from M&K, two main differences are observed:

- Damage progression rate is higher for the HRL experiments, specially for Case 03. This is due to a steeper slope and to the fact that depth-limited conditions are avoided and, thus, the highest waves of the spectrum also attack the model and favor a steeper shape of the damage progression curve.
- Damage deviation is also higher for the HRL experiments. That might be a consequence of three main reasons; firstly, in the HRL experiments 6 sections were studied in comparison with the 2 sections analyzed by M&K; secondly, damage was defined as a mean value of the parameter *S* for each section in the HRL experiments whereas M&K considered each profile measurement on the same section as independent values of *S*; and thirdly, it seems reasonable to relate depth limited waves to less variability in damage evolution because wave breaking in the transition ramp concentrates the band of energy interacting with the structure.

The results from fitting Eq.3 into the damage progression curve of Figure 10 are summarized in Table 7. Figure 12 shows the optimum damage progression approximation (HRL_01). Additionally, two representative optimization cases are graphically presented in Figure 13: case HRL_02, where the geometrical parameter *b* is fixed to 0.5, and case HRL_05, where the geometrical parameter *b* is fixed to 0.25 (matching the one used by M&K in their model).

Table 7. Optimized parameters of Eq.3 based on the experimental results of the HRL's damage tests. Bold characters are fixed values in the optimization process

| CASE	γ	b	k (N_{S1})	k (N_{S2})	r (N_{S1})	r (N_{S2})	μ_0	σ_0	Error
HRL_01	-8.750	0.285	0.3898	2.3515	2882.0	35833.	0.8909	0.0127	0.2984
HRL_02	-8.448	**0.500**	0.0064	0.0187	0.3250	1.1921	0.5790	0.0487	0.3074
HRL_03	-8.767	**0.400**	0.0261	0.0976	7.2927	42.724	0.6573	0.0089	0.3036
HRL_04	-8.901	**0.300**	0.2480	1.3930	1086.9	11538.	0.8706	0.1911	0.2990
HRL_05	-7.792	**0.250**	1.1215	8.5582	28790.	652752	0.7840	0.1056	0.3052
HRL_06	**0.000**	0.569	0.0009	0.0049	0.1089	0.4268	0.3253	0.0107	0.3253
HRL_07	**0.000**	**0.500**	0.0013	0.0091	0.4663	0.0812	0.3326	0.0000	0.3326
HRL_08	**0.000**	**0.400**	0.0024	0.0307	7.9089	0.0886	0.3410	1.3808	0.3410
HRL_09	**0.000**	**0.300**	0.0071	0.2070	743.16	0.0922	0.3676	2.5646	0.3676
HRL_10	**0.000**	**0.250**	0.0169	0.9029	24037.	0.0574	0.3921	0.1716	0.3921
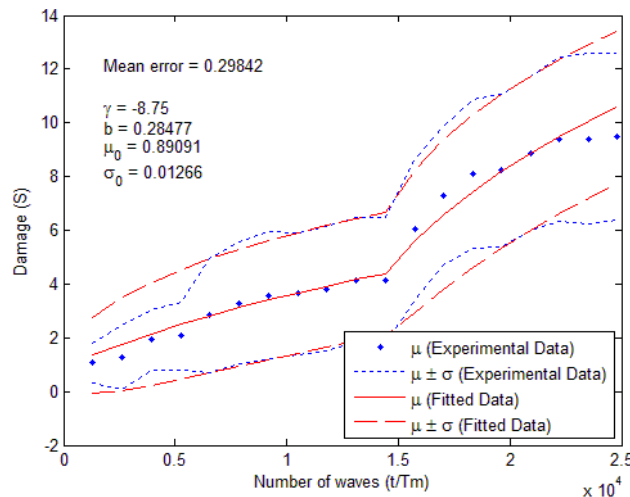
Figure 12. Graphic results from the fitting process of the optimum case (HRL_01), based on the experimental results from Figure 10.
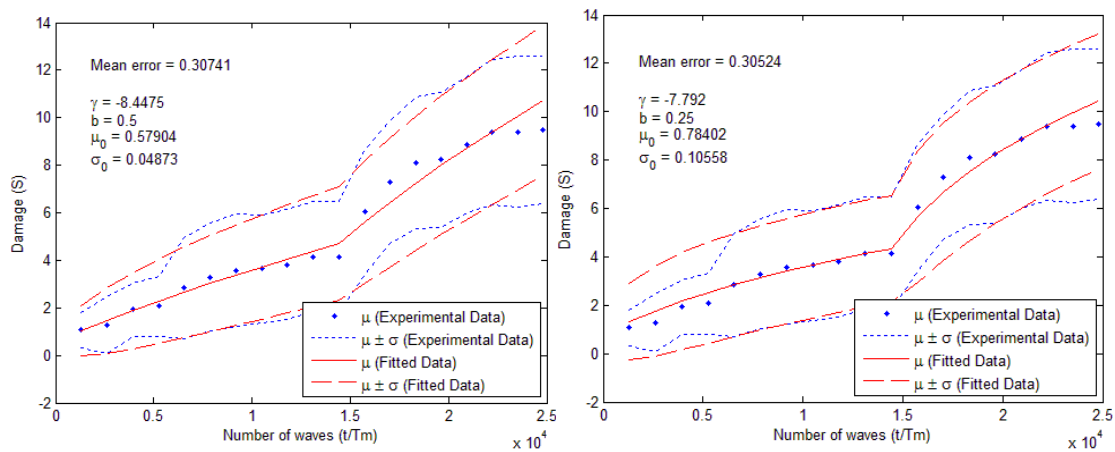
Figure 13. Graphic results from the fitting process of Case HRL_02 (left) and Case HRL_5 (right), based on the experimental results from Figure 10.

After analyzing these results, analogous conclusions to the ones stated after the DPPM calibration using M&K's results can be derived. The goodness of fit is slightly worse for this case. Again, based on Figure 12, it can be concluded that the lesser the magnitude of *b* is, the faster damage tends to stabilize. While the optimum value of *b* was 0.29 for the Initial Section (lower water depth) and 0.21 for the Final Section (higher water depth) of Series A of M&K, in this case a value around 0.30 is more appropriate. The highest damage progression rate and damage deviation in the HRL's experimental damage progression curve seems to be related to higher magnitudes of the wave action parameters, *k* and *r*. Finally, a proper magnitude of the location parameter (γ) was appreciated to be specially relevant for enhancing the goodness of fit with the lower values of *b*. The location parameter shows a reasonable constant magnitude among the different optimized cases for each experimental Series.

4. CONCLUSIONS

In the present study, the stochastic nature of the hydraulic instability of rubble mound breakwaters has been addressed. The conclusions can be summarized in the following points:

- As it was stated by many authors, damage development and progression highly depends on placement. Even using the same laboratory technician and allocating the armor units with a similar porosity (31% to 34%), different structural behaviors have been reported for the 6 similar quarry-stones rubble mound sections, after exposing them for the same wave cases. This is associated with a different interlocking of the granular system, as an unavoidable part of the construction process.

- Damage has a spatial component that might not be completely characterized with the well-known quantitative damage level parameter (*S*) proposed by Broderick and Ahrens (1982). In addition, a lack of standards in damage measurement and analysis is being perceived, which, in fact, is fundamental for reproducibility, repeatability and comparison between experiments.

- The stochastic nature of damage has been traditionally linked to a normal distribution. However, according to the suggestions from Castillo et al. (2012), damage has been proven not to follow a normal distribution, but transformed damage $D_{trans}=(D-\gamma)^{1/b}$ does instead. Based on assumptions of general validity and with a comprehensive probabilistic approach, they proposed the DPPM of Eq.3 which permits, not only to predict the mean trend of damage progression, but also the whole PDF.

- Each armor unit has a different mechanism of damage initiation, different interaction with waves or even a different way of defining what is considered as "damage". Therefore both damage definition and parameters of the DPPM need to be defined independently for each armor unit. The present paper presents some initial calibrations with quarry-stones, using the results from M&K experiments and further experiments carried out at the HRL of Madrid. The influence of the different variables in the model has been analyzed but more research is needed for conclusive results.

- The employed methodology for damage measurement and model calibration in laboratory is applicable for prototype conditions, but prototype monitoring is needed for that purpose. Thanks to the recent advances and affordability of non-intrusive drones and scanning/photogrammetric technologies, Port's Authorities have nowadays tools to monitor their structures in order to

evaluate the state of the breakwater after a certain storm. That would help to develop a field database for enhancing laboratory results.

5. ACKNOWLEDGMENTS

6. REFERENCES

Ahrens, J. P. and McCartney, B. L. 1975. Wave period effect on the stability of riprap. *Proc. Civ. Engineering. in the Oceans III*, ASCE, 1019-1034.

Burcharth, H.F. 1997. Reliability based design of coastal structures. Advances in Coastal and Ocean Engineering. ed. Phillip L-F Liu. Vol. 3 World Scientific Publishing Co Pte Ltd. 145-214.

Cabrerizo, M.A., Molina, R., Matutano, C., and Llana, A. 2010. Control of porosity, reflection and transmission coefficients using polymeric porous media and their application in testing physical models. *Proceedings of 3rd International Conference on the Application of Physical Modeling to Port and Coastal Protection*, Barcelona.

Campos, A., Castillo, C. and Molina, R. 2010. Optimizing breakwater design considering the system of failure modes. *Proc, 32nd Int. Conf. on Coastal Engrg*, ASCE. Shanghai, China.

Campos, A. 2014. A methodology for the analysis of damage progression in rubble mound breakwaters. PhD-Thesis, E.T.S.I. de Caminos, Canales y Puertos de Ciudad Real, University of Castilla-La Mancha (Spain).

Carver, R. D. and Wright, B. L. 1991. An investigation of random variations in the stability response of stone armored, rubble mound breakwaters. Technical Report CERC-91-17, U. S: Army Engineer Waterways Experiment Station, Vicksburg, MS.

Castillo, E., Losada, M., Mínguez, R., Castillo, C., and Baquerizo, A. 2004. Optimal Engineering Design Method that Combines Safety Factors and Failure Probabilities: Application to Rubble-Mound Breakwaters. *J. Waterw. Port Coast. Ocean Eng*. 130, 77–88.

Castillo, C., Mínguez, R., Castillo, E., and Losada, M.A. 2006. An optimal engineering design method with failure rate constraints and sensitivity analysis. Application to composite breakwaters. *Coastal Engineering*. 53, 1–25.

Castillo, C., Castillo, E., Fernández-Canteli, A., Molina, R., and Gómez, R. 2012. Stochastic Model for Damage Accumulation in Rubble-Mound Breakwaters Based on Compatibility Conditions and the Central Limit Theorem. *J. Waterway, Port, Coastal, Ocean Eng*., 138(6), 451–463.

CIRIA. 2007. The Rock Manual. The use of rock in hydraulic engineering (second edition)

De Castro, E. 1933. Diques de Escollera. *Revista de Obras Públicas*, Madrid. 183-185. (in Spanish)

Gómez-Martín, M.E. and Medina, R. 2004. Wave-to-wave exponential estimation of armor damage progression. *Coastal Engineering*. 3592-3604.

Hald, T. 1998. Wave Induced Loading and Stability of Rubble Mound Breakwaters. Series Paper No 18. PhD-thesis, Hydraulics and Coastal Engineering Laboratory, Aalborg University.

Hudson, R. Y. 1958. Design of quarry-stone cover layers for rubble-mound breakwaters. Research Report 2-2, U. S. Army Engineer Waterways Experiment Station, Vicksburg, MS.

Iribarren, R. 1938. Una fórmula para el cálculo de los diques en escollera (a formula for the calculation of rock-fill dikes). Technical Report HE-116-295, *Revista de Obras Públicas*, Madrid, Spain. Translated by D. Heinrich, Fluid Mech. Lab., Univ. of California, Berkeley, CA.

Kaku, S., Kobayashi, N., and Ryu, C.R. 1991. Design formulas for hydraulic stability of rock slopes under irregular wave attack. *Proc. of 38th Japanese Coast. Engrg. Conf*, JSCE, 661-665 (in Japanese)

Losada, M.A. and Giménez-Curto, L.A. 1979. The Joint Effect of the Wave Height and Period on the Stability of Rubble Mound Breakwaters Using Iribarren's Number. *J. of Coastal Eng*.,3. 77-96.

Medina, J.R. 1992. A robust armor design to face uncertainties. *Proc. 23rd Coastal Engineering Conference*, ASCE, New York, 1371-1384.

Medina, J.R., Hudspeth, R.T., and Fassardi, C. 1994. Breakwater armor damage due to wave groups. *J. Waterway, Port, Coastal, Ocean Eng*., ASCE, 120(2), 179-198.

Medina, J. R. 1996. Wave climate simulation and breakwater stability. *Proc, 25th Int. Conf. on Coastal Engrg*, ASCE. 1789-1802.

Melby, J.A., y Kobayashi, N. 1998. Progression and variability of damage on rubble mound breakwaters. *J. Waterway, Port, Coastal, Ocean Eng*., 124(6), 286-294.

Melby, J. A., and Kobayashi, N. 1999. Damage progression and variability on breakwater trunks. *Proc. Coastal Structures '99* Vol 1, 309-315.

Melby, J. A. 1999. Damage progression on rubble-mound breakwaters. Technical Report CHL-99-17, US Army Corps of Engineers, Waterways

Mínguez, R., Castillo, E., Castillo, C., and Losada, M.A. 2006. Optimal cost design with sensitivity analysis using decomposition techniques. Application to composite breakwaters. *Structural Safety*. 28, 321–340.

Negro, V., Varela, O., García, J. H.,López, J. S., 2001. Diques Verticales. *Colegio de Ingenieros de Caminos, Canales y Puertos ed*. (in Spanish)

Oumeraci, H., 1994, Review and analysis of vertical breakwater failures - lessons learned. *Coastal Engineering*, vol. 22, 3-29.

Oumeraci, H. · Allsop, N.W.H. · De Groot, M.B. · Crouch, R.S. · Vrijling, J.K. 1999. PROVERBS: Probabilistic design tools for vertical breakwaters.

Puertos del Estado. 2001. ROM 0.0-01, General procedure and requirements in the design of harbour and maritime structures.

Teisson, C. 1990. Statistical Approach of Duration of Extreme Storms: Consequences on Breakwater Damages. *Proc, 22nd Int. Conf. on Coastal Engrg*., ASCE, 1851-1860.

Thompson D.M. and Shuttler R.M. 1975. Rip-rap design for wind wave attack. Report No. EX 707, Wallingford, UK.

U.S. Army Corps of Engineers, 2002, CEM: Coastal Engineering Manual. EM 110-2-1100 (Part VI) Change 3 (28 Sep 2011)

Van der Meer, J. W. 1985. Stability of rubble mound revetments and breakwaters under random wave attack. *Developments in Breakwaters*, ICE. Proc. Breakwaaters '85 Conference, London, Chap. 5.

Vidal, C, Losada, M.A. and Medina, R. 1991. Stability of Mound Breakwater's Head and Trunk. *J. Waterway, Port, Coastal, Ocean Eng*., Vol. 117, No. 6, 570-587.